Supplemental Materials

Nanopore sequencing. Long-read genomic sequencing was performed using the third generation Oxford Nanopore MinION MkIb (Isolates 1-30) and GridION X5 (Isolates 31-40; Oxford, England) sequencing instruments. Genomic DNA was extracted from pure cultures using the DNeasy PowerBiofilm Kit (Qiagen, Hilden, Germany). Each Nanopore sequencing library was prepared using 5 µg of DNA with the 1D ligation kit (SQK-LSK108, Oxford Nanopore Technologies) using R9.4 flowcells (FLO-MIN106). A single isolate was run per flowcell. MinKNOW software was used to collect sequencing data. Three separate analysis pipelines were performed: (1) a real-time Nanopore analysis approach, (2) an assembly-based Nanopore approach, and (3) an Illumina Pilon-corrected approach. The run statistics and the whole genome assembly parameters are summarized in the Supplemental File Run & Assembly Statistics. Sequencing data for this study were deposited in the Sequencing Read Archive (SRA; BioProject number: PRJNA496461), and genome assemblies submitted to NCBI.

Nanopore real-time approach. For the real-time analysis approach, the Oxford Nanopore Technology “What’s In My Pot” (WIMP)(1) and Metrichor’s Antimicrobial Resistance Mapping Application (ARMA) (2) real-time analysis tools were run in parallel to both sequencing and base-calling. WIMP uses a customized pipeline applying the Centrifuge metagenomic classifier to the sequencing reads. ARMA aligns sequencing reads to the Comprehensive Antimicrobial Database (CARD)(3), identifying antimicrobial resistance (AMR) gene hits.

Nanopore assembly-based approach. For the assembly-based approach, Albacore v2.1.3 was used to base-call. Raw data were corrected, trimmed, and assembled using Canu v1.6(4) using default parameters. Genome size was assumed to be 5.3Mb. For isolates that did not assemble under default parameters, either read quality restrictions were relaxed or minimum

overlap requirements were shortened as suggested by the software documentation. Assembled contigs were screened for resistance genes using Abricate (htts://github.com/tseemann/abricate), a tool that uses alignment to search for resistance gene sequences from several database including ResFinder, CARD, ARG-ANNOT, and the NCMI AMR Reference Gene Database. ResFinder results were evaluated in this study(5). In a separate experiment, we were able to build high quality genomes from nanopore electrical data in under 6 hours using a machine with 36 cores and 72GB RAM. Thirteen random blocks of 4000 reads were sampled and taken through basecalling, assembly and polishing. Conservatively, it takes at most an hour to reach 52,000 reads on a typical run.

Illumina sequencing. WGS was also conducted using Illumina MiSeq short-read sequencing to increase assembly accuracy (Illumina, San Diego, California). A drawback with Illumina sequencing is the turn-around time as sequencing alone requires between 19-24 hours for 300 cycles. As the ultimate goal would be to use Nanopore sequencing alone for both resistance gene and chromosomal mutation identification, in the current analysis, the Pilon-corrected assemblies were not meant to supplant or supplement Nanopore sequencing but rather to serve as a reference standard to determine the accuracy of Nanopore sequencing results. Approximately 100-500 ng of gDNA was used to prepare sequencing libraries using the Nextera Flex Kit. The each Illumina library was then sequenced using both v2 2x150 and v3 2x75 reagents on an Illumina Miseq. These reads were used to correct the more error prone Nanopore assembly with the Pilon v1.22 software package in conjunction with the short-read aligner Bowtie2 v2.2.6.

Analysis for Detection of Chromosomal Mutations. Both Nanopolished Nanopore assemblies and hybrid Illumina-corrected Nanopore assemblies were further evaluated for chromosomal mutations presumed to confer resistance. These included truncations in the outer

membrane proteins OmpK35 and OmpK36 as a consequence of premature stop codons resulting in carbapenem resistance and *gyrA* (DNA gyrase; nucleotide positions 247-249 & 259-261) and *parC* (topoisomerase IV; nucleotide positions 238-240 & 250-252) point mutations that encoded amino acid changes resulting in fluoroquinolone resistance. Additionally, mutations in *mgrB*, the negative regulator of the two-component regulatory system that renders polymixins ineffective were evaluated.

Coding sequences encompassing chromosomal mutations of interest were extracted from the genome of the *K. pneumoniae* ATCC 13883 strain and used to align with genomic assemblies using minimap2 (6). Code written in C++ was developed for parsing alignment data and mutations, evaluating their impact on amino acid translation based on resulting codon changes(7). Substitutions causing synonymous codons were reported as such, and frameshift mutations were followed downstream to report premature stop codons. Additionally, the program analyzed DNA sequences surrounding mutation sites looking for homopolymers or methylation motifs specific for *K. pneumoniae* as indicators of potential sequencing issues rather than mutations in the genome.

Predicted correlations between resistance genes/mutations and AST results. Predictions of resistance were performed without reference to phenotypic data. The correlation of resistance genes and sequence variants with anticipated AST results for the evaluated antibiotics was determined based on reference gene databases and the published literature(8-26). For associations for which ambiguity existed, the following rules were established *a priori*:

- SHV 2be extended-spectrum β-lactamase enzymes were assumed to inactivate ceftriaxone and cefepime if they contained G238S or E240K mutations(19, 27)
- The relative contributions of porins OmpK35 and/or OmpK36 truncations to β-lactam resistance have not been well established(13, 28-32). There appears to be consensus

that when premature stop codons are present for both, in conjunction with ESBLs or AmpC cephalosporinases, carbapenem resistance is likely.

- Aminoglycoside modifying enzymes (AMEs)- including aminoglycoside N-acetyltransferases [AACs], aminoglycoside O-nucleotidyltransferases [ANTs], or aminoglycoside O-phosphotransferases [APHs] are anticipated to confer resistance to gentamicin and tobramycin (17). Correlations between the number of different enzymes produced and the association with aminoglycoside resistance are not well defined. After exploratory analysis (Table 1), we predicted that when four or more AMEs were present, gentamicin and tobramycin resistance was likely.
- The AME *aac(6')Ib-cr* was also evaluated for its contribution to ciprofloxacin resistance(17).
- Ribosomal RNA methyltransferases (*armA, rmtA, rmtB, rmtC, rmtD*, or *rmtE*) are expected to confer resistance to amikacin, gentamicin, and tobramycin (18).
- Plasmid-encoded quinolone resistance genes *qnrB, qnrS, aac(6')Ib-cr* and *oqxAB* (chromosomally encoded) were predicted to cause low-level fluoroquinolone resistance, but not frank resistance (16, 33, 34).

Single *gyrA* or *parC* mutations were not predicted to cause fluoroquinolone resistance but two-step *gyrA* mutations or the presence of both *gyrA* and *parC* mutations translating to amino acid changes were expected to result in fluoroquinolone resistance (33, 34).

References

1. **Juul S IF, Hurst A, Dai X, Wright A, Kulesha E, Perrett R, Turner DJ.** 2016. What's in my pot? Real-time species identification on the MinION. https://doi.org/10.1101/030742. Accessed October 17th, 2018.
2. **Real-time detection of antibiotic-resistance genes Https://publication-admin.nanoporetech/2016/05/18/real-time-detection-of-antibiotic-resistance-genes-poster/. Accessed October 17th.**
3. **Jia B, Raphenya AR, Alcock B, Waglechner N, Guo P, Tsang KK, Lago BA, Dave BM, Pereira S, Sharma AN, Doshi S, Courtot M, Lo R, Williams LE, Frye JG, Elsayegh T, Sardar D, Westman EL, Pawlowski AC, Johnson TA, Brinkman FS, Wright GD, McArthur AG.** 2017. CARD 2017: expansion and model-centric curation of the comprehensive antibiotic resistance database. Nucleic Acids Res **45:**D566-D573.
4. **Koren S, Walenz BP, Berlin K, Miller JR, Bergman NH, Phillippy AM.** 2017. Canu: scalable and accurate long-read assembly via adaptive k-mer weighting and repeat separation. Genome Res **27:**722-736.
5. **Zankari E, Hasman H, Cosentino S, Vestergaard M, Rasmussen S, Lund O, Aarestrup FM, Larsen MV.** 2012. Identification of acquired antimicrobial resistance genes. J Antimicrob Chemother **67:**2640-2644.
6. **Li H.** 2018. Minimap2: pairwise alignment for nucleotide sequences. Bioinformatics doi:10.1093/bioinformatics/bty191.
7. **Pairwise alignments of DNA sequences. https://github.com/gpertea/pwasmAccessed October 17th.**
8. **Bush K, Jacoby GA.** 2010. Updated functional classification of beta-lactamases. Antimicrob Agents Chemother **54:**969-976.
9. **Bush K, Jacoby GA, Medeiros AA.** 1995. A functional classification scheme for beta-lactamases and its correlation with molecular structure. Antimicrob Agents Chemother **39:**1211-1233.
10. **Jacoby GA.** 2009. AmpC beta-lactamases. Clin Microbiol Rev **22:**161-182, Table of Contents.
11. **Naas T, Poirel L, Nordmann P.** 2008. Minor extended-spectrum beta-lactamases. Clin Microbiol Infect **14 Suppl 1:**42-52.
12. **Evans BA, Amyes SG.** 2014. OXA beta-lactamases. Clin Microbiol Rev **27:**241-263.
13. **Zhang Y, Jiang X, Wang Y, Li G, Tian Y, Liu H, Ai F, Ma Y, Wang B, Ruan F, Rajakumar K.** 2014. Contribution of beta-lactamases and porin proteins OmpK35 and OmpK36 to carbapenem resistance in clinical isolates of KPC-2-producing Klebsiella pneumoniae. Antimicrob Agents Chemother **58:**1214-1217.
14. **Chen FJ, Lauderdale TL, Ho M, Lo HJ.** 2003. The roles of mutations in gyrA, parC, and ompK35 in fluoroquinolone resistance in Klebsiella pneumoniae. Microb Drug Resist **9:**265-271.
15. **Vetting MW, Hegde SS, Wang M, Jacoby GA, Hooper DC, Blanchard JS.** 2011. Structure of QnrB1, a plasmid-mediated fluoroquinolone resistance factor. J Biol Chem **286:**25265-25273.
16. **Kim HB, Wang M, Park CH, Kim EC, Jacoby GA, Hooper DC.** 2009. oqxAB encoding a multidrug efflux pump in human clinical isolates of Enterobacteriaceae. Antimicrob Agents Chemother **53:**3582-3584.
17. **Ramirez MS, Tolmasky ME.** 2010. Aminoglycoside modifying enzymes. Drug Resist Updat **13:**151-171.
18. **Galimand M, Courvalin P, Lambert T.** 2012. RmtF, a new member of the aminoglycoside resistance 16S rRNA N7 G1405 methyltransferase family. Antimicrob Agents Chemother **56:**3960-3962.

19. **Liakopoulos A, Mevius D, Ceccarelli D.** 2016. A Review of SHV Extended-Spectrum beta-Lactamases: Neglected Yet Ubiquitous. Front Microbiol **7:**1374.
20. **B-Lactamase Classification and Amino Acid Sequences for TEM S, and OXA Extended-Spectrum and Inhibitor Resistant Enzymes. http://www.lahey.org/studies/ Accessed October 17th, 2018.**
21. **Tarnberg M, Nilsson LE, Monstein HJ.** 2009. Molecular identification of (bla)SHV, (bla)LEN and (bla)OKP beta-lactamase genes in Klebsiella pneumoniae by bi-directional sequencing of universal SP6- and T7-sequence-tagged (bla)SHV-PCR amplicons. Mol Cell Probes **23:**195-200.
22. **Bonnet R.** 2004. Growing group of extended-spectrum beta-lactamases: the CTX-M enzymes. Antimicrob Agents Chemother **48:**1-14.
23. **Fevre C, Passet V, Weill FX, Grimont PA, Brisse S.** 2005. Variants of the Klebsiella pneumoniae OKP chromosomal beta-lactamase are divided into two main groups, OKP-A and OKP-B. Antimicrob Agents Chemother **49:**5149-5152.
24. **Roberts MC.** 2005. Update on acquired tetracycline resistance genes. FEMS Microbiol Lett **245:**195-203.
25. **Fu Y, Zhang W, Wang H, Zhao S, Chen Y, Meng F, Zhang Y, Xu H, Chen X, Zhang F.** 2013. Specific patterns of gyrA mutations determine the resistance difference to ciprofloxacin and levofloxacin in Klebsiella pneumoniae and Escherichia coli. BMC Infect Dis **13:**8.
26. **Poirel L, Naas T, Nordmann P.** 2010. Diversity, epidemiology, and genetics of class D beta-lactamases. Antimicrob Agents Chemother **54:**24-38.
27. **Howard C, van Daal A, Kelly G, Schooneveldt J, Nimmo G, Giffard PM.** 2002. Identification and minisequencing-based discrimination of SHV beta-lactamases in nosocomial infection-associated Klebsiella pneumoniae in Brisbane, Australia. Antimicrob Agents Chemother **46:**659-664.
28. **Shelburne SA, Kim J, Munita JM, Sahasrabhojane P, Shields RK, Press EG, Li X, Arias CA, Cantarel B, Jiang Y, Kim MS, Aitken SL, Greenberg DE.** 2017. Whole-Genome Sequencing Accurately Identifies Resistance to Extended-Spectrum beta-Lactams for Major Gram-Negative Bacterial Pathogens. Clin Infect Dis **65:**738-745.
29. **Tsai YK, Fung CP, Lin JC, Chen JH, Chang FY, Chen TL, Siu LK.** 2011. Klebsiella pneumoniae outer membrane porins OmpK35 and OmpK36 play roles in both antimicrobial resistance and virulence. Antimicrob Agents Chemother **55:**1485-1493.
30. **Landman D, Bratu S, Quale J.** 2009. Contribution of OmpK36 to carbapenem susceptibility in KPC-producing Klebsiella pneumoniae. J Med Microbiol **58:**1303-1308.
31. **Jiang X, Espedido BA, Partridge SR, Thomas LC, Wang F, Iredell JR.** 2009. Paradoxical effect of Klebsiella pneumoniae OmpK36 porin deficiency. Pathology **41:**388-392.
32. **Domenech-Sanchez A, Martinez-Martinez L, Hernandez-Alles S, del Carmen Conejo M, Pascual A, Tomas JM, Alberti S, Benedi VJ.** 2003. Role of Klebsiella pneumoniae OmpK35 porin in antimicrobial resistance. Antimicrob Agents Chemother **47:**3332-3335.
33. **Ruiz J, Pons MJ, Gomes C.** 2012. Transferable mechanisms of quinolone resistance. Int J Antimicrob Agents **40:**196-203.
34. **Jacoby GA.** 2005. Mechanisms of resistance to quinolones. Clin Infect Dis **41 Suppl 2:**S120-126.

Supplemental Table 1: Anticipated antibiotic susceptibility results for 40 *Klebsiella pneumoniae* isolates based on resistance determinants detected by Nanopore sequencing technology real-time analysis; first column for each antibiotic indicates presumed activity and second column for each antibiotic indicates *in vitro* activity based on broth microdilution results with green indicating susceptible and red indicating intermediate or resistant; number on bottom represents percent agreement between presumed and *in vitro* activity

#	Resistance determinants identified with real-time Nanopore [# of allelic variants identified for each gene]*	Missing resistance determinants based on pilon-corrected Illumina data	Piperacillin-tazobactam		Ceftriaxone		Cefepime		Ertapenem		Meropenem		Amikacin		Gentamicin		Ciprofloxacin		Colistin		Doxycycline		TMP-SMX	
1	*bla*$_{SHV}$[75]; *bla*$_{CTX-M}$[34]; *bla*$_{OXA}$[2]; *bla*$_{KPC}$[18]; *aac*[7]; qnr[6]; *oqxA*[1]; *oqxB*[1]; *aadA[4];* su[1]l; *dfr*[1]	Two-step *gyrA* mutations; OmpK36 truncation																						
2	*bla*$_{SHV}$[81] (*bla*$_{LEN}$); *bla*$_{CTX-M}$[31]; *bla*$_{OXA}$[2]; *bla*$_{TEM}$[104]; *bla*$_{KPC}$[11]; *qnr*[7]; *aac*[13]; *aadA*[9]; *dfr*[1]	*oqxA*; *oqxB*; *tet(B)*; *aph(6")-Id*; aph(3')-Ia; *sul1*; *sul2*; one-step *gyrA* mutation; *parC* mutation; OmpK35 and OmpK36 truncation																						
3	*bla*$_{SHV}$[25]; *oqxA*[1]; *oqxB*[1]	OmpK36 truncation																						
4	*bla*$_{SHV}$[57]; *bla*$_{TEM}$[48]; *bla*$_{KPC}$[4]; *aadA*[4]	*oqxA*; *oqxB*; *sul1*; one-step *gyrA* mutation, *parC* mutation; OmpK36 truncation																						
5	*bla*$_{SHV}$[70]; *oqxA*[1]; *oqxB*[1]	OmpK36 truncation																						

6	*bla*$_{SHV}$[5]; *bla*$_{TEM}$[1]; *bla*$_{OXA}$[2]; *bla*$_{KPC}$[14]; *aac*[3]; *oqxA*[1]; *oqxB*[1]; *aph[2]; aadA*[1]*; sul*[1]; *dfr*[1]	two-step *gyrA* mutation; *parC* mutation; OmpK35 and OmpK36 truncation	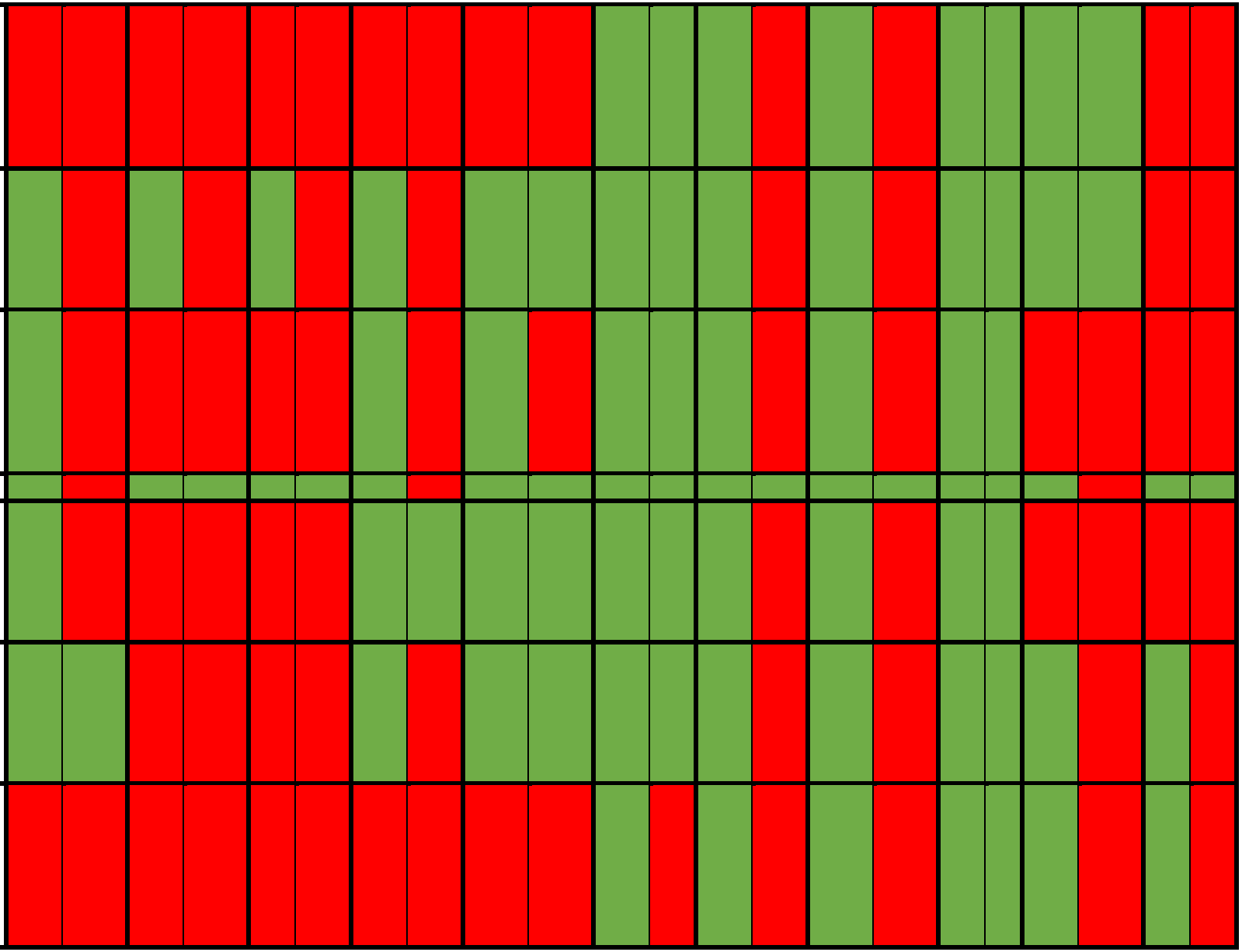
7	*bla*$_{OXA}$[4]; *bla*$_{SHV}$[19]; *oqxA*[1]; *oqxB*[1]; *aac*[1]*; aadA*[3]*; sul*[1]; *dfr*[1]	two-step *gyrA* mutation; *parC* mutation; OmpK35 and OmpK36 truncation	
8	*bla*$_{OXA}$[2]; *bla*$_{TEM}$[3]; *bla*$_{CTX-M}$[27]; *bla*$_{SHV}$[30]; *aac*[6]*; oqxA*; *oqxB*; *qnr*[12]; *aph*[2]*; sul*[2]*; dfr*[1]*; tet*[1]	one-step *gyrA* mutation; *parC* mutation; *aacA4*; OmpK36 truncation	
9	*bla*$_{SHV}$(*bla*$_{LEN}$)[94]	*oqxA*; *oqxB*	
10	*bla*$_{OXA}$[3]; *bla*$_{CTX-M}$[31]; *bla*$_{TEM}$[6]; *bla*$_{SHV}$[57]; *aac*[7]; *qnr[21]; oqxA*[1]; *oqxB*[1]; *aph*[2]*; su[2]; dfr*[1]*; tet*[1]	OmpK36 truncation	
11	*bla*$_{CTX-M}$[18]; *bla*$_{TEM}$[15]; *bla*$_{SHV}$[56]*; aac*[3]	*oqxA; oqxB; sul2; dfrA14; aph(6)-Id; aph(3")-Ib;* OmpK36 truncation	
12	*bla*$_{TEM}$[58]; *bla*$_{SHV}$[32]; *bla*$_{CTX-M}$[6]; *bla*$_{NDM}$[5]; *bla*$_{OXA}$[2]; *qnr*[13]; *aac*[8]*; aph*[1]*; aadA*[3]	*rmtf*; *oqxA*; *oqxB*; OmpK35 truncation; *sul1*; *dfrA12*; one-step *gyrA* mutation; *parC* mutation	

13	*bla*$_{OXA}$[2]; *bla*$_{CTX-M}$[7]; *bla*$_{TEM}$[1]; *bla*$_{SHV}$[8]; *bla*$_{NDM}$[6]; *qnr*[1]; *oqxA*[1]; *oqxB*[1]; *aadA*[1]; *aac*[2]; *sul*[1]	OmpK35 and OmpK36 truncation; one-step *gyrA* mutation; *parC* mutation																					
14	bla$_{SHV}$[89]; bla$_{OXA}$[3]; bla$_{TEM}$[18]; bla$_{CTX-M}$[23]; bla$_{KPC}$[18]; *aac*[20]; *aadA*[10]; *tet*[4]; *dfrA*[1]; *sul*[2]	*oqxA*; *oqxB*; *tet(B)*; *aph(6)-Id*; *aph(3")-Ib*; one-step *gyrA* mutation; *parC* mutation; OmpK35 and OmpK36 truncation																					
15	*bla*$_{SHV}$[87]; *oqxA*[1]; *oqxB*[1]; *qnr*[6]; *sul*[1]; *dfr*[1]; *tet*[1]	*tet(A)*; *tet(D)*; OmpK36 truncation; *mgrB* mutation																					
16	*bla*$_{SHV}$[116]; *bla*$_{KPC}$[18]; *aac*[17]; *oqxA*[1]; *oqxB*[1]; *aadA*[9]; *aac*[18]; *sul*[1]	two-step *gyrA* mutations; *parC* mutation; Ompk35 and Ompk36 truncation																					
17	*bla*$_{CTX-M}$[42]; *bla*$_{KPC}$[18]; *bla*$_{SHV}$[62]; *bla*$_{TEM}$[23]; *bla*$_{OXA}$[22]; *oqxA*[1]; *oqxB*; *aac*[22]; *aph*[9]; *tet*[1]; *sul*[3] *dfr*[4]	two-step *gyrA* mutations; OmpK36 truncation																					
18	*bla*$_{CTX-M}$[23]; *bla*$_{TEM}$[36]; *bla*$_{KPC}$[8]; *bla*$_{SHV}$	*oqxA*; *oqxB*; *tet(A)*; two-step *gyrA* mutation; *parC* mutation; OmpK36 truncation																					

19	*bla*$_{TEM}$[20]; *bla*$_{SHV}$[52]; *bla*$_{OXA}$[1]; *bla*$_{KPC}$[1]; *qnr*[1]; *aac*[2]; *aadA*[3]	*oqxA*; *oqxB*; OmpK36 truncation; one-step *gyrA* mutation; *parC* mutation; dfrA14	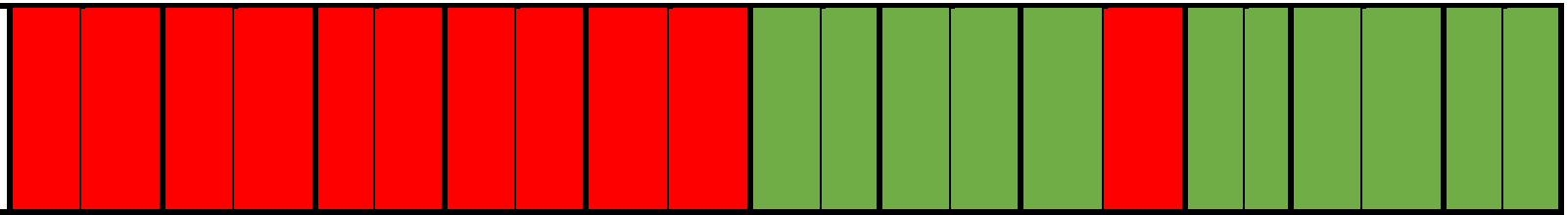
20	*bla*$_{SHV}$[108]; *bla*$_{TEM}$[111]; *bla*$_{KPC}$[11]; *aac*[13]; *aadA*[10]	*bla*$_{OXA-9}$; *oqxA*; *oqxB*; one-step *gyrA* mutation; *parC* mutation; OmpK35 mutation; OmpK36 truncation; *aph(3')-Ia; aph(4)-Ia; sul1; dfrA12*	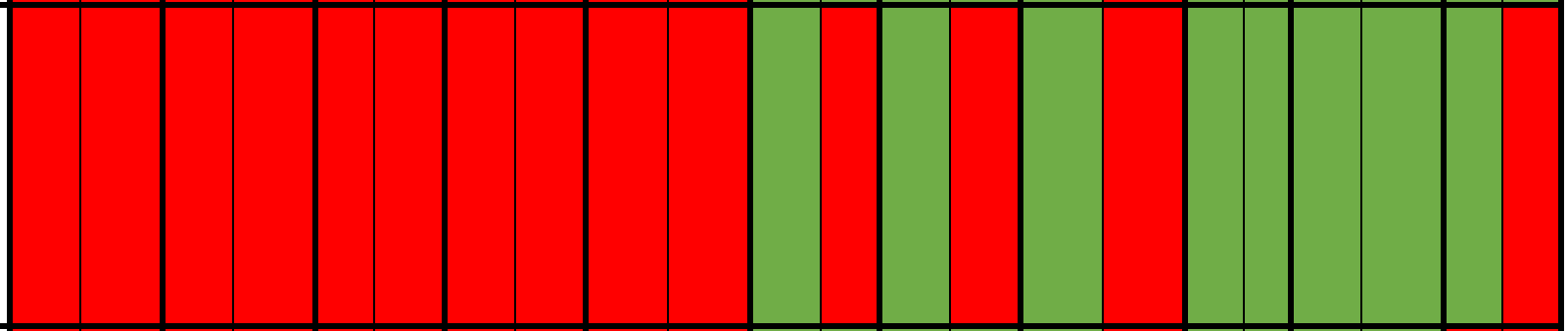
21	*bla*$_{KPC}$[18]; *bla*$_{SHV}$[98]; *bla*$_{TEM}$[21]; *aac*[17]; *aadA*[8]; *oqxA*[1]; *oqxB*[1]; *sul*[1]; *dfrA*[1]	one-step *gyrA* mutation; *parC* mutation; OmpK35 and OmpK36 truncation	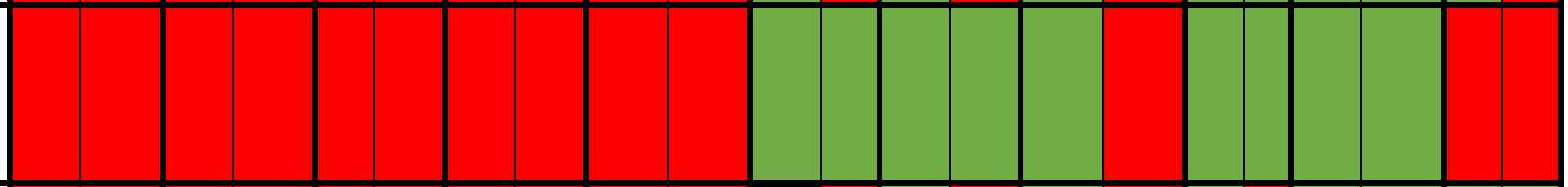
22	*bla*$_{TEM}$[22]; *bla*$_{KPC}$[18]; *bla*$_{OXA}$[1]; *bla*$_{SHV}$[41]; *qnr*[10]; *oqxA*[1]; *oqxB*[1]; *aac*[9]; *aadA*[5]	one-step *gyrA* mutation; *parC* mutation; *mgrB* mutation; OmpK36 truncation	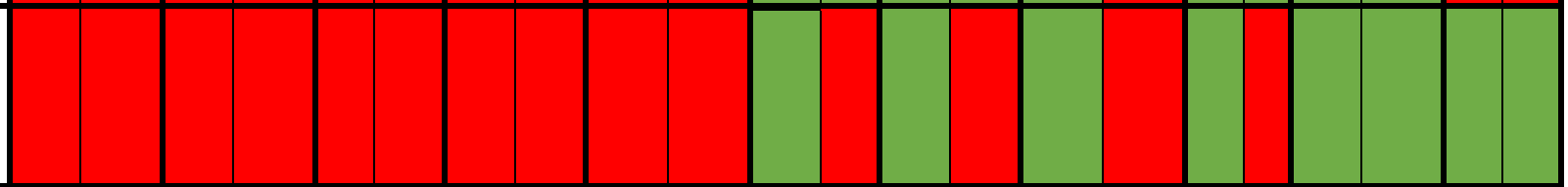
23	*bla*$_{KPC}$[16]; *bla*$_{SHV}$[56]; *bla*$_{OXA}$[2]; *bla*$_{TEM}$[8]; *aac*[15]; *oqxA*; *oqxB*; aph[1]; *aadA*[7]; *sul*[2]; *dfrA*[1]	one-step *gyrA* mutation; *parC* mutation; OmpK35 and OmpK36 truncation	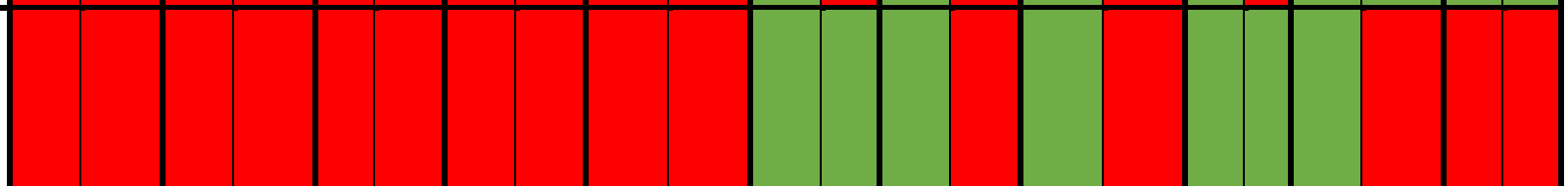
24	*bla*$_{TEM}$[64]; *bla*$_{CTX-M}$[35]; *bla*$_{DHA}$[6]; *bla*$_{SHV}$[67]; *qnr*[1]; *aac*[1]; *aadA*[7]	*rmtB*; *oqxA*; *oqxB*; one-step *gyrA* mutation; OmpK36	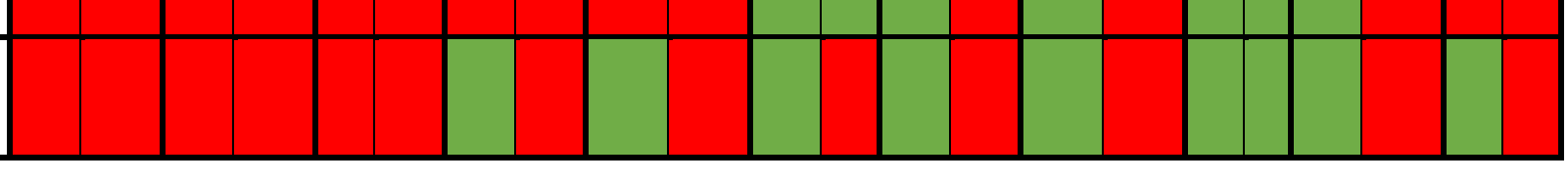

		truncation; *tet(A)*; *tet(G)*; *aph(3')-Ia; aph(3")-Ib; aph(3)-IId; aph(6)-Id; sul1*; *sul2*; *dfrA12*; *dfrA1*																					
25	*bla*$_{SHV}$[72]; *oqxA*[1]; *oqxB*[1]	OmpK36 truncation																					
26	*bla*$_{SHV}$[68]; *bla*$_{KPC}$[18]; *oqxA*[1]; *oqxB*[1]; *aac*[11]; aadA[8]	One-step *gyrA* mutation; *parC* mutation; OmpK35 and OmpK36 truncation																					
27	*bla*$_{SHV}$[59]; *bla*$_{TEM}$[41]; *bla*$_{KPC}$[6]; *aac*[8]; *aadA*[5]	*bla*$_{OXA}$; *oxqA*; *oqxB*; OmpK35 and OmpK36 truncation; aph(3')-Ia; one-step *gyrA* mutation; *parC* mutation; *sul1*; *dfrA12*																					
28	*bla*$_{SHV}$[94]; *bla*$_{TEM}$[14]; *bla*$_{OXA}$[2]; *bla*$_{KPC}$[18]; *aac*[14]; *oqxA*[1]; *oqxB*[1]; *aph*[2]; aad[5]; sul[2]; *dfrA*[1]	one-step *gyrA* mutation; *parC* mutation; OmpK35 and OmpK36 truncation; premature stop codon in *mgrB*																					
29	*bla*$_{SHV}$[29]; *bla*$_{NDM}$[7]; *bla*$_{CTX-M}$[22]; *bla*$_{CMY}$[39]; *qnr*[12]; *aac*[10]; *aadA*[5]; *sul*[1]	*rmtf*; *oqxA*; *oqxB*; one-step *gyrA* mutation; *parC* mutation; OmpK35 truncation; *aacA4; aph(3')-VIa; dfrA12*																					

30	*bla*$_{SHV}$[45]; *bla*$_{TEM}$[38]; *bla*$_{OXA}$[6]; *bla*$_{KPC}$[9]; *aac*[2]; *aadA*[5];	*oqxA*; *oqxB*; *qnrS1*; two-step *gyrA* mutation; *parC* mutation; *phoP* mutation; OmpK36 truncation; *aph(3')-Ia; sul1*; *sul3*; *dfrA12*	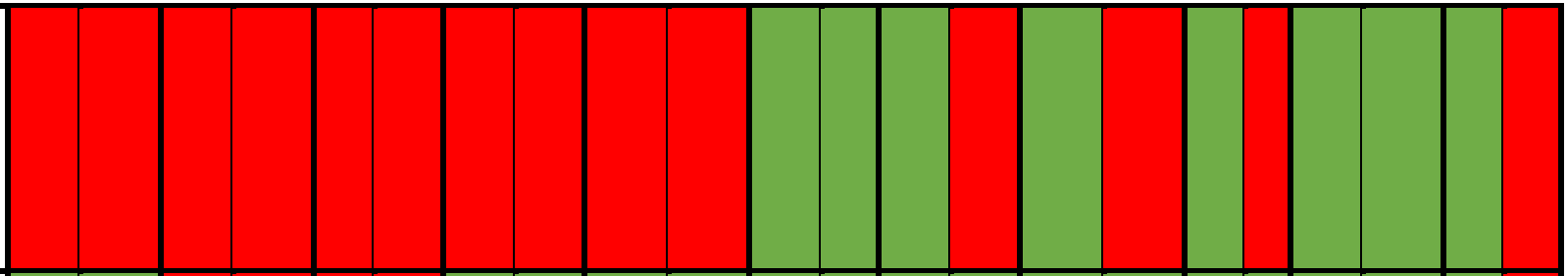
31	*bla*$_{CTX-M}$[19]; *bla*$_{TEM}$[22]; *bla*$_{SHV}$[36]; *qnr*[11]	*oqxA*; *oqxB*; OmpK36 truncation; *aph(6)-Id; aph(3")-Ib; sul2; dfrA14*	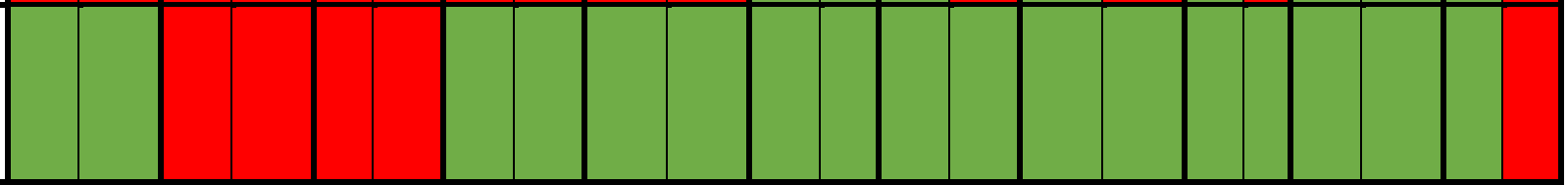
32	*bla*$_{OXA}$[3]; *bla*$_{SHV}$[60]; *bla*$_{CTX-M}$[23]; *bla*$_{TEM}$[20]; *qnr*[12]; *aac*[2]	*oqxA*; *oqxB*; *tet(A)*; *aph(6)-Id; aph(3")-Ib; sul2*; dfrA14; OmpK36 truncation	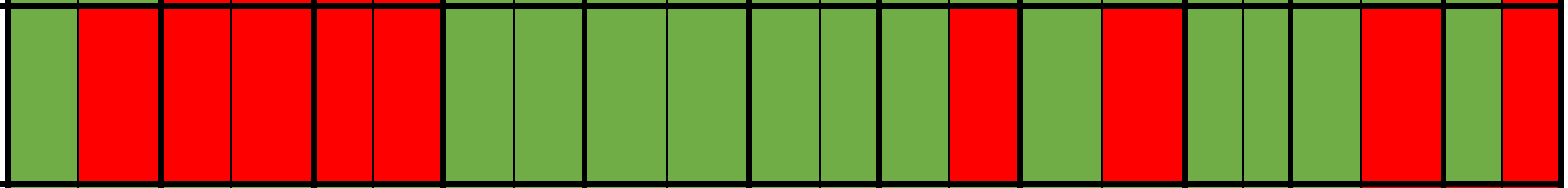
33	*bla*$_{SHV}$[25](*bla*$_{LEN}$[25]; *oqxA*[1]; *oqxB*[1]; *sul2*[1]; *dfrA14*[1]	OmpK36 truncation; *tet(D)*	
34	*bla*$_{SHV}$[23]; *oqxA*[1]; *oqxB*[1]	OmpK36 truncation	
35	*bla*$_{SHV}$[24]; *oqxA*[1]; *oqxB*[1]	OmpK36 truncation	
36	*bla*$_{SHV}$[22]; *oqxA*[1]; *oqxB*[1]	ant(2")-Ia; OmpK36 truncation	
37	*bla*$_{TEM}$[41]; *bla*$_{KPC}$[8]; *bla*$_{SHV}$[85]; *ant*[1]	*qnrS1*; OmpK36 truncation	
38	*bla*$_{OKP}$[9]; *bla*$_{TEM}$[12]; *bla*$_{SHV}$[1]; *oqxA*; *oqxB*; *sul*; *dfr*	*tet(D)*; OmpK36 truncation	

39	bla_{SHV}[62]; *oqxA*[1]; *oqxB*[1]	OmpK36 truncation																				
40	bla_{SHV}[23]; *oqxA*[1]; *oqxB*[1]	OmpK36 truncation																				
Overall agreement			**80%**		**93%**		**95%**		**83%**		**93%**		**78%**		**45%**		**30%**		**93%**		**63%**		**68%**	

*****Due to the raw sequencing error rate for the real-time Nanopore sequencing analysis, multiple variants of resistance genes are frequently identified by ARMA. For example, for the result "bla_{KPC}[3]," three allelic variants would be identified bla_{KPC-2}, bla_{KPC-3}, $bla_{KPC-5.}$

195

196

197

198

199

200

201

202

203

204

205

206

207

208

209

210

Supplemental Table 2: Anticipated antibiotic susceptibility results for 40 *Klebsiella pneumoniae* isolates based on resistance determinants detected by Nanopore sequencing technology with assembly; first column for each antibiotic indicates presumed activity and second column for each antibiotic indicates *in vitro* activity based on broth microdilution results with green indicating susceptible and red indicating intermediate or resistant; number on bottom represents percent agreement between presumed and *in vitro* activity

#	Resistance determinants identified with Nanopore sequencing with assembly	Missing resistance determinants based on pilon-corrected Illumina data	Piperacillin-tazobactam		Ceftriaxone		Cefepime		Ertapenem		Meropenem		Amikacin		Gentamicin		Ciprofloxacin		Colistin		Doxycycline		TMP-SMX	
1	*bla*$_{SHV-1}$; *bla*$_{CTX-M-15}$; *bla*$_{OXA-1}$; *bla*$_{KPC-3}$; OmpK36 truncation; *qnrS1*; *oqxA; oqxB*; two-step *gyrA* mutations; *aac(6')-Ib-cr; aadA2; sul1*; *dfrA12*	None																						
2	*bla*$_{SHV-11}$; *bla*$_{CTX-M-15}$; *bla*$_{OXA-1}$; *bla*$_{TEM-1}$; *bla*$_{KPC-2}$; OmpK35 and OmpK36 truncation; *qnrB1*; *oqxA; oqxB;* one-step *gyrA* mutation; parC mutation; *tet(B)*; *aadA2; aph(3')-Ia; aac(3)-IId; aac(6')-Ib-cr; aadA2; aac(3)-IIa; aph(6")-Id; aaA1; aac(6')-Ib; sul1; sul2; dfrA12; dfrA30*	None																						
3	*bla*$_{SHV-11}$; *oqxA*; *oqxB*; Ompk36 truncation	None																						
4	*bla*$_{SHV-11}$; *bla*$_{TEM-1}$; *bla*$_{KPC-3}$; OmpK36 truncation; *oqxA*; *oqxB*; one-step *gyrA*	None																						

	mutation; *parC* mutation; *aadA2*; *sul1*		
5	bla_{SHV-11}; Ompk36 truncation; *oqxA*; *oqxB*	None	
6	bla_{SHV-11}; bla_{TEM-1}; bla_{OXA-9}; bla_{KPC-3}; aac(6')-Ib-cr; *oqxA*; *oqxB*; two-step *gyrA* mutations; *parC* mutation; OmpK35 and OmpK36 truncation; *aph(3")-Ib; aph(6)-Id; aadA1; aac(6)-Ib; sul2*; *dfrA14*	None	
7	bla_{OXA-2}; bla_{SHV-11}; bla_{SHV-30}; bla_{SHV-12}; *oqxA*; *oqxB*; aac(6')-Ib-cr; two-step *gyrA* mutations; *parC* mutation; OmpK35 and Ompk36 truncation; *aadA2; aacA4; sul1*; *dfrA12*; *fosA*	None	
8	bla_{OXA-1}; bla_{TEM-1}; $bla_{CTX-M-15}$; bla_{SHV-28}; OmpK36 truncation; aac(6')-Ib-cr; *oqxA*; *oqxB*; *qnrB1*; one-step *gyrA* mutation; *parC* mutation; *tet(A)*; *aph(3")-Ib; aph(6)-Id; aac(3)-IIa*; *sul2; dfrA14*	bla_{OXA-47}; *aacA4*	
9	bla_{LEN-12}; bla_{SHV-11}; OmpK36 truncation; *oqxA*; *oqxB*	None	

10	*bla*$_{OXA-1}$; *bla*$_{CTX-M-15}$; *bla*$_{TEM-1}$; *bla*$_{SHV-101}$; OmpK36 truncation; aac(6')-Ib-cr; *qnrB1*; *oqxA*; *oqxB*; *tet(A)*; *aac(3)-IIa; aac(6)-Id; aac(3")-Ib; aph(6)-Id; aph(3")-Ib*	*aacA4*																						
11	*bla*$_{CTX-M-15}$; *bla*$_{TEM-1}$; *bla*$_{SHV-11}$; OmpK36 truncation; *aac(6')-Ib-cr*; *oqxA*; *oqxB*; *aph(6)-Id*; *aph(3")-Ib*; *sul2*; *dfrA14*	None																						
12	*bla*$_{TEM-1}$; *bla*$_{SHV-1}$; *bla*$_{CTX-M-15}$; *bla*$_{NDM-1}$; *bla*$_{OXA-48}$; OmpK35 truncation; *qnrB1*; *rmtf*; aac(6')-Ib-cr; aph(3')-VIa; *oqxA*; *oqxB*; one-step *gyrA* mutation, *parC* mutation; *sul1*; *dfrA12*	None																						
13	*bla*$_{OXA-1}$; *bla*$_{CTX-M-15}$; *bla*$_{TEM-1}$; *bla*$_{SHV-11}$; *bla*$_{OXA-9}$; *bla*$_{NDM-1}$; aac(6')-Ib-cr; *qnrS1*; oqxA; oqxB; one-step *gyrA* mutation; *parC* mutation; OmpK35 and OmpK36 truncation; *aadA1*; *aac(6')-Ib*; *sul1*	None																						
14	bla$_{SHV-11}$; bla$_{SHV-2}$; bla$_{OXA-1}$; bla$_{TEM-1}$; bla$_{CTX-M-15}$; bla$_{KPC-2}$; *oqxA*; *oqxB*; *aac(6')-Ib-cr*; *aac(6')-Ib*; *aph(3')-Ia*; *aadA1*; *aadA2*; *aac(3)-IId*;	None																						

	aac(6')-Ib-cr; *aac(3')-IIa*; *aph(6)-Id*; *aph(3")-Ib*; one-step *gyrA* mutation; *parC* mutation; OmpK35 and OmpK36 truncation; *tet(B); sul2; dfrA30*																							
15	bla_{SHV-11}; bla_{SHV-1}; OmpK36 truncation; *oqxA*; *oqxB*; *qnrB2*; *mgrB* mutation; *tet(A); tet(D)*; *sul1*; *dfrA25*	None																						
16	bla_{SHV-11}; bla_{KPC-3}; bla_{SHV-12}; aac(6')-Ib-cr; oqxA; *oqxB*; two-step *gyrA* mutations; *parC* mutation; OmpK35 and OmpK36 truncation; *aadA2; aadA1; aac(6')-Ib; sul3*	bla_{KPC-9}																						
17	$bla_{CTX-M-15}$; bla_{KPC-2}; bla_{SHV-28}; bla_{TEM-1B}; bla_{OXA-1}; OmpK36 truncation; *oqxA*; *oqxB*; aac(6')-Ib-cr; two-step *gyrA* mutations; *aph(3")-Ib*; *aph(6)-Id*; *aac(3)-IIa*; *tet(A)*; *sul2*; *dfrA14*	None																						
18	$bla_{CTX-M-15}$; bla_{TEM-1B}; bla_{KPC-2}; bla_{SHV-28}; OmpK36 truncation; *oqxA*; *oqxB*; one-step *gyrA* mutation; *parC* mutation; *tet(A)*	One-step *gyrA* mutation																						
19	bla_{KPC-3}; bla_{TEM-1}; bla_{OXA-9}; bla_{SHV-11};																							

	oqxA; *oqxB*; *qnrS1*; *aac(6')-Ib-cr*; one-step *gyrA* mutation; *parC* mutation; *aadA1*; *aac(6')-Ib*; OmpK36 truncation; *dfrA14*																							
20	bla_{SHV-11}; bla_{OXA-9}; bla_{KPC-2}; bla_{TEM-1}; OmpK35 and OmpK36 truncation; *aac(6')-Ib-cr*; *oqxA*; *oqxB*; one-step *gyrA* mutation; *parC* mutation; *aph(3')-Ia*; *aadA2*; *aadA1*; *aac(6')-Ib*; *aac(3)-IVa*; *aph(4)-Ia*; *aadA15*; *sul1*; *dfrA12*	None																						
21	bla_{KPC-3}; bla_{SHV-12}; bla_{TEM-1}; bla_{SHV-11}; OmpK35 and OmpK36 truncation; aac(6')-Ib-cr; *oqxA*; *oqxB*; one-step *gyrA* mutation; *parC* mutation; *aadA2*; *aac(6')-Ib*; *sul1*; *dfrA12*	None																						
22	bla_{TEM-1}; bla_{KPC-3}; bla_{OXA-9}; bla_{SHV-11}; OmpK36 truncation; *qnrB19*; *oqxA*; *oqxB*; *aac(6')-Ib-cr*; one-step *gyrA* mutation; *parC* mutation; *mgrB* mutation; *aac(3)-IId*; *aac(6')-Ib*; *aadA1*	None																						
23	bla_{KPC-2}; bla_{SHV-11}; bla_{OXA-9}; bla_{TEM-1}; *aac(6')-Ib-cr*; *oqxA*;	None																						

	oqxB; one-step *gyrA* mutation; *parC* mutation; OmpK35 and Ompk36 truncation; *aac(6')-Ib*; aadA2; aac(3)-IVa; aph(4)-Ia; aadA2; aadA1; *sul1*; *sul3*; *dfrA12*																							
24	bla_{TEM-1}; $bla_{CTX-M-14}$; bla_{DHA-1}; bla_{SHV-11}; OmpK36 truncation; *qnrB4*; *oqxA*; *oqxB*; one-step *gyrA* mutation; *tet(A)*; *tet(G)*; rmtB; *aph(3")-Ib; aph(3')-Ia*; *aac(3)-IId*; *aph(6)-Id*; *aph(3)-IId*; *aadA2*; *aadA5*; *sul1*; *sul2*; *dfrA12*; *dfrA1*	None																							
25	bla_{SHV-11}; OmpK36 truncation; *oqxA*; *oqxB*	None																							
26	bla_{SHV-11}; bla_{KPC-2}; *oqxA*; *oqxB*; one-step *gyrA* mutation; *parC* mutation; OmpK35 and OmpK36 truncation; *aac(6')-Ib*; *aadA2*; *aadA1*; *aadA24*	None																							
27	bla_{SHV-11}; bla_{TEM-1}; bla_{OXA-9}; bla_{KPC-2}; *oqxA*; *oqxB*; aac(6')-Ib-cr; one-step *gyrA* mutation; *parC* mutation; *aph(3')-Ia*; *aadA2*; *aac(6')-Ib*; *sul1*; *dfrA12*	None																							

28	*bla*$_{SHV-12}$; *bla*$_{TEM-1}$; *bla*$_{OXA-9}$; *bla*$_{KPC-3}$; *bla*$_{SHV-11}$; OmpK35 and OmpK36 truncation; aac(6')-Ib-cr; *oqxA*; *oqxB*; one-step *gyrA* mutation; *parC* mutation; *aac(6')-Ib*; *aph(3")-Ib*; *aadA1*; *sul2*; *dfrA14*; premature stop codon in *mgrB*	None																					
29	*bla*$_{SHV-1}$; *bla*$_{NDM-1}$; *bla*$_{CTX-M-15}$; *bla*$_{CMY-4}$; OmpK35 truncation; *qnrB1; aac(6')-Ib-cr*; *oqxA*; *oqxB*; one-step *gyrA* mutation; *parC* mutation; rmtf; *aacA4*; *aph(3')-VIa*; *aadA2*; *sul1*; *dfrA12*	None																					
30	bla$_{SHV-11}$; bla$_{TEM-1}$; bla$_{OXA-2}$; bla$_{KPC-3}$; OmpK36 truncation; *phoP* mutation; *aac(6')-Ib-cr*; *oqxA*; *oqxB*; *qnrS1*; two-step *gyrA* mutation; *parC* mutation; *aadA8b; aadA1; aadA2; aac(3)-IIa; aacA4; aac(3)-IIa; aacA4; aph(3')-Ia; sul1*; *sul3*; *dfrA12*	*aadA8*																					
31	*bla*$_{CTX-M-15}$; *bla*$_{TEM-1}$; *bla*$_{SHV-83}$; OmpK36 truncation; *oqxA*; *oqxB*; *qnrB1; aph(6)-Id; aph(3")-Ib; sul2; dfrA14*																						

32	*bla*$_{OXA-1}$; *bla*$_{SHV-11}$; *bla*$_{CTX-M-15}$; *bla*$_{TEM-1B}$; OmpK36 truncation; *oqxA*; *oqxB; qnrB1; aac(6')-Ib-cr; tet(A); aph(6)-Id; aph(3")-Ib; sul2; dfrA14*																					
33	*bla*$_{LEN-12}$; *bla*$_{SHV-1}$; OmpK36 truncation; *oqxA*; *oqxB*; *tet(D)*; *sul2*; *dfrA14*	None																				
34	*bla*$_{SHV-71}$; OmpK36 truncation; *oqxA*; *oqxB*	None																				
35	*bla*$_{SHV-1}$; OmpK36 truncation; *oqxA*; *oqxB*	None																				
36	*bla*$_{SHV-36}$; OmpK36 truncation; *oqxA*; *oqxB*; *ant(2")-Ia*	None																				
37	*bla*$_{TEM-1}$; *bla*$_{KPC-3}$; *bla*$_{SHV-26}$; *bla*$_{SHV-30}$; OmpK36 truncation; *ant(2")-Ia; qnrS1*	None																				
38	*bla*$_{OKP-B2}$; *bla*$_{TEM-1}$; *bla*$_{SHV-122}$; OmpK36 truncation; *oqxA*; *oqxB*; *tet(D)*; *sul2*; *dfrA26*	None																				
39	*bla*$_{SHV-62}$; OmpK36 truncation; *oqxA*; *oqxB*	None																				
40	*bla*$_{SHV-83}$; OmpK36 truncation; *oqxA*; *oqxB*	None																				
Overall agreement			**85%**		**95%**		**98%**		**85%**		**95%**		**85%**		**93%**		**98%**		**98%**		**80%**	**93%**

211

212

Supplemental Table 3: Anticipated antibiotic susceptibility results for 40 *Klebsiella pneumoniae* isolates based on resistance determinants detected by Nanopore sequencing technology with assembly and Pilon-corrected Illumina data; first column for each antibiotic indicates presumed activity and second column for each antibiotic indicates *in vitro* activity based on broth microdilution results with green indicating susceptible and red indicating non-susceptible; number on bottom represents percent agreement between presumed and *in vitro* activity

#	Resistance mechanisms identified	Piperacillin-tazobactam		Ceftriaxone		Cefepime		Ertapenem		Meropenem		Amikacin		Gentamicin		Ciprofloxacin		Colistin		Doxycycline		TMP-SMX	
1	*bla*$_{SHV-1}$; *bla*$_{CTX-M-15}$; *bla*$_{OXA-1}$; *bla*$_{KPC-3}$; OmpK36 truncation; *qnrS1*; *oqxA; oqxB*; two-step *gyrA* mutations; *aac(6')-Ib-cr*; *aadA2*; *sul1*; *dfrA12*																						
2	*bla*$_{SHV-11}$; *bla*$_{CTX-M-15}$; *bla*$_{OXA-1}$; *bla*$_{TEM-1}$; *bla*$_{KPC-2}$; OmpK35 and OmpK36 truncation; *qnrB1*; *oqxA; oqxB;* one-step *gyrA* mutation; parC mutation; *tet(B)*; *aadA2; aph(3')-Ia; aac(3)-IId; aac(6')-Ib-cr; aadA2; aac(3)-IIa; aph(6")-Id; aaA1; aac(6')-Ib; sul1; sul2; dfrA12; dfrA30*																						
3	*bla*$_{SHV-11}$; *oqxA*; *oqxB*; OmpK36 truncation																						
4	*bla*$_{SHV-11}$; *bla*$_{TEM-1}$; *bla*$_{KPC-3}$; OmpK36 truncation; *oqxA*; *oqxB*; one-step *gyrA* mutation; *parC* mutation; *aadA2*; *sul1*																						
5	*bla*$_{SHV-11}$; OmpK36 truncation; *oqxA*; *oqxB*																						
6	bla$_{SHV-11}$; bla$_{TEM-1}$; bla$_{OXA-9}$; bla$_{KPC-3}$; *aac(6')-Ib-cr*; *oqxA*; *oqxB*; two-step *gyrA* mutations; *parC* mutation; OmpK35 and OmpK36 truncation; *aph(3")-Ib; aph(6)-Id; aadA1; aac(6)-Ib; sul2; dfrA14*																						
7	*bla*$_{OXA-2}$; *bla*$_{SHV-11}$; *bla*$_{SHV-30}$; *bla*$_{SHV-12}$; *oqxA*; *oqxB*; aac(6')-Ib-cr; two-step *gyrA* mutations; *parC* mutation; OmpK35 and OmpK36 truncation; *aadA2; aacA4; sul1*; *dfrA12*; *fosA*																						
8	*bla*$_{OXA-1}$; *bla*$_{OXA-47}$; *bla*$_{TEM-1}$; *bla*$_{CTX-M-15}$; *bla*$_{SHV-28}$; OmpK36 truncation; *aac(6')-*																						

	Ib-cr; *oqxA*; *oqxB*; *qnrB1*; one-step *gyrA* mutation; *parC* mutation; *tet(A)*; *aph(3")-Ib; aph(6)-Id; aac(3)-IIa;* aacA4*; sul2; dfrA14*	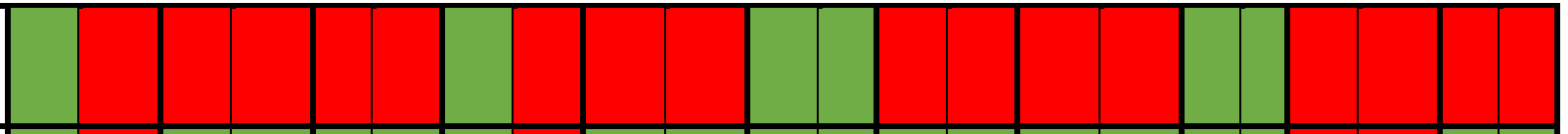
9	bla_{LEN-12}; bla_{SHV-11}; OmpK36 truncation; *oqxA*; *oqxB*	
10	bla_{OXA-1}; $bla_{CTX-M-15}$; bla_{TEM-1}; $bla_{SHV-101}$; OmpK36 truncation; aac(6')-Ib-cr; *qnrB1*; *oqxA*; *oqxB*; *tet(A)*; *aacA4; aac(3)-IIa; aac(6)-Id; aac(3")-Ib; aph(6)-Id; aph(3")-Ib*	
11	$bla_{CTX-M-15}$; bla_{TEM-1}; bla_{SHV-11}; OmpK36 truncation*; aac(6')-Ib-cr; oqxA; oqxB; aph(6)-Id; aph(3")-Ib; sul2; dfrA14*	
12	bla_{TEM-1}; bla_{SHV-1}; $bla_{CTX-M-15}$; bla_{NDM-1}; bla_{OXA-48}; OmpK35 truncation; *qnrB1*; *rmtf*; *aac(6')-Ib-cr; aph(3')-VIa; oqxA*; *oqxB*; one-step *gyrA* mutation, *parC* mutation; *sul1*; *dfrA12*	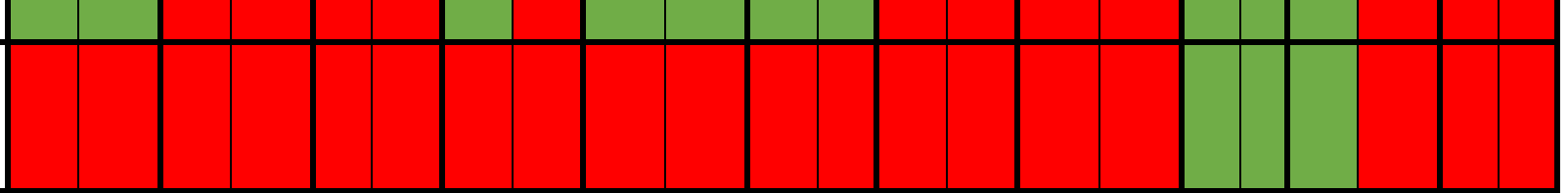
13	bla_{OXA-1}; $bla_{CTX-M-15}$; bla_{TEM-1}; bla_{SHV-11}; bla_{OXA-9}; bla_{NDM-1}; *aac(6')-Ib-cr; qnrS1*; oqxA; oqxB; one-step *gyrA* mutation; *parC* mutation; OmpK35 and OmpK36 truncation; *aadA1*; *aac(6')-Ib*; *sul1*	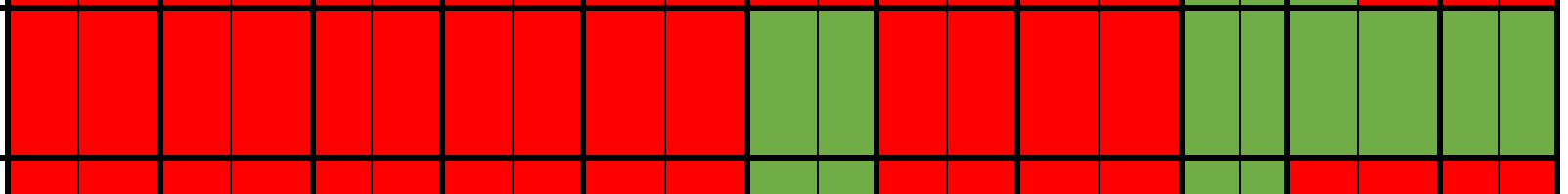
14	bla_{SHV-11}; bla_{SHV-2}; bla_{OXA-1}; bla_{TEM-1}; $bla_{CTX-M-15}$; bla_{KPC-2}; *oqxA*; *oqxB*; *aac(6')-Ib-cr; aac(6')-Ib; aph(3')-Ia; aadA1; aadA2; aac(3)-IId; aac(6')-Ib-cr; aac(3')-IIa; aph(6)-Id; aph(3")-Ib*; one-step *gyrA* mutation; *parC* mutation; OmpK35 and OmpK36 truncation; *tet(B); sul2; dfrA30*	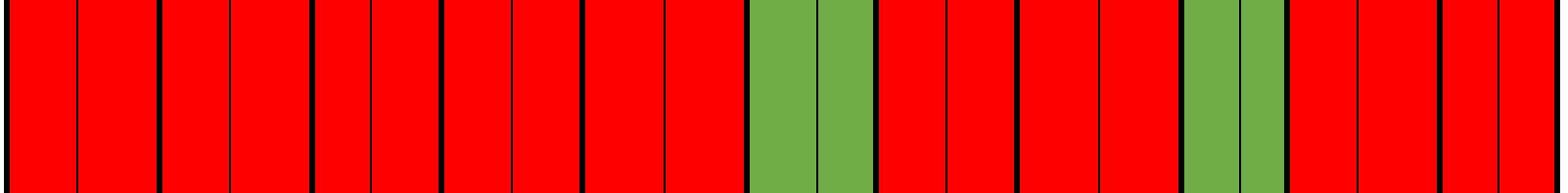
15	bla_{SHV-11}; bla_{SHV-1}; OmpK36 truncation; *oqxA*; *oqxB*; *qnrB2*; *mgrB* mutation; *tet(A); tet(D)*; *sul1*; *dfrA25*	
16	bla_{SHV-11}; bla_{KPC-3}; bla_{KPC-9}; bla_{SHV-12}; *aac(6')-Ib-cr*; oqxA; *oqxB*; two-step *gyrA* mutations; *parC* mutation; OmpK35 and OmpK36 truncation; *aadA2; aadA1; aac(6')-Ib; sul3*	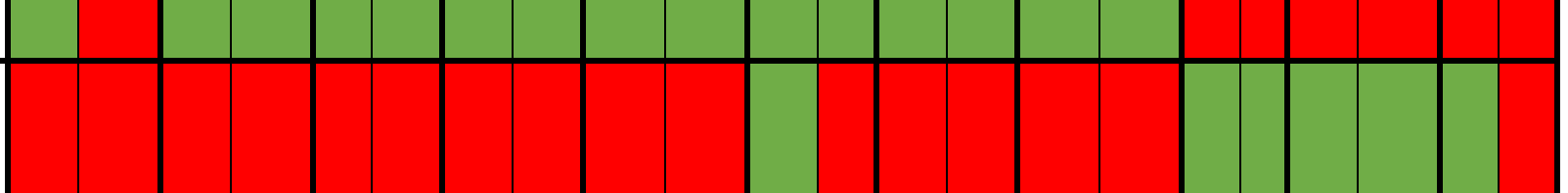

17	*bla*$_{CTX-M-15}$; *bla*$_{KPC-2}$; *bla*$_{SHV-28}$; *bla*$_{TEM-1B}$; *bla*$_{OXA-1}$; OmpK36 truncation; *oqxA*; *oqxB*; *aac(6')-Ib-cr*; two-step *gyrA* mutations; *aph(3")-Ib; aph(6)-Id; aac(3)-IIa; tet(A)*; *sul2*; *dfrA14*	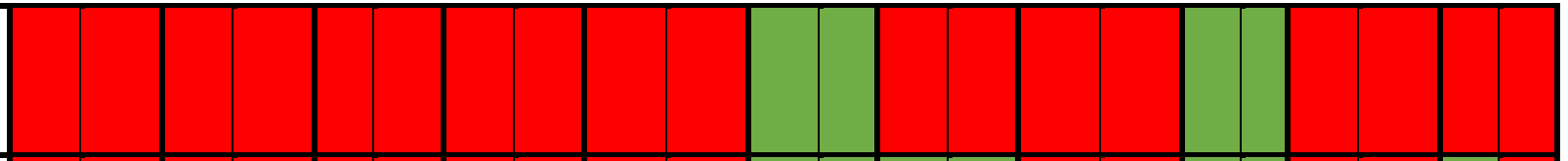
18	*bla*$_{CTX-M-15}$; *bla*$_{TEM-1B}$; *bla*$_{KPC-2}$; *bla*$_{SHV-28}$; OmpK36 truncation; *oqxA*; *oqxB*; two-step *gyrA* mutations; *parC* mutation; *tet(A)*	
19	*bla*$_{KPC-3}$; *bla*$_{TEM-1}$; *bla*$_{OXA-9}$; *bla*$_{SHV-11}$; *oqxA*; *oqxB*; *qnrS1*; *aac(6')-Ib-cr*; one-step *gyrA* mutation; *parC* mutation; *aadA1*; *aac(6')-Ib*; *dfrA14*; OmpK36 truncation	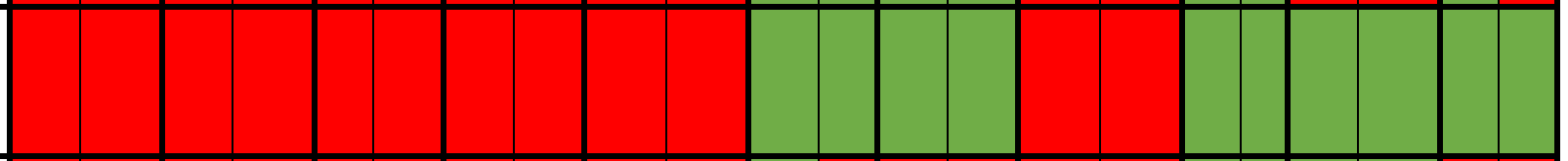
20	*bla*$_{SHV-11}$; *bla*$_{OXA-9}$; *bla*$_{KPC-2}$; *bla*$_{TEM-1}$; OmpK35 and OmpK36 truncation; *aac(6')-Ib-cr*; *oqxA*; *oqxB*; one-step *gyrA* mutation; *parC* mutation; *aph(3')-Ia; aadA2; aadA1; aac(6')-Ib; aac(3)-IVa; aph(4)-Ia; aadA15*; *sul1*; *dfrA12*	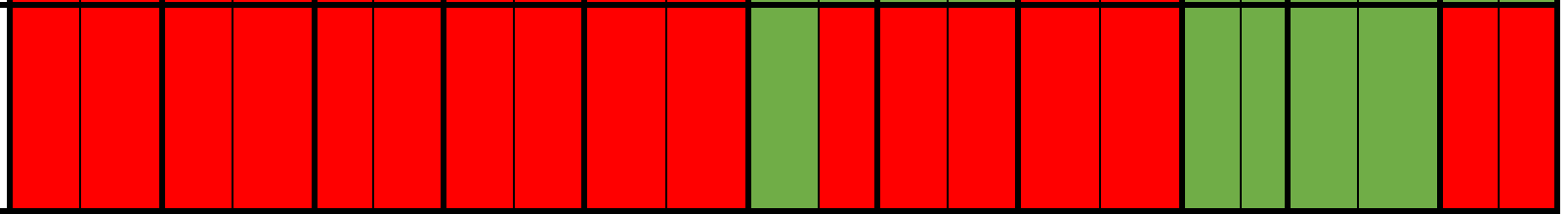
21	*bla*$_{KPC-3}$; *bla*$_{SHV-12}$; *bla*$_{TEM-1}$; *bla*$_{SHV-11}$; OmpK35 and OmpK36 truncation; *aac(6')-Ib-cr; oqxA*; *oqxB*; one-step *gyrA* mutation; *parC* mutation; *aadA2; aac(6')-Ib; sul1*; *dfrA12*	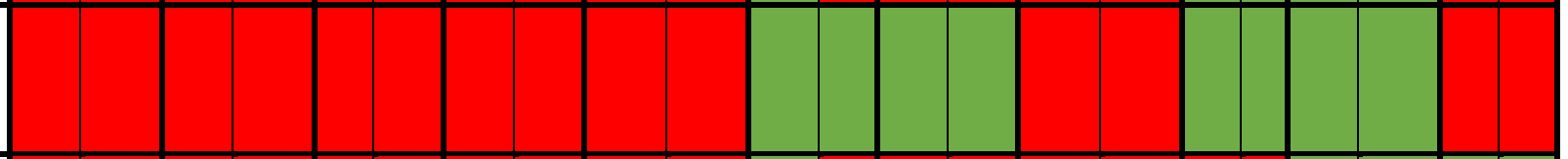
22	*bla*$_{TEM-1}$; *bla*$_{KPC-3}$; *bla*$_{OXA-9}$; *bla*$_{SHV-11}$; OmpK36 truncation; *qnrB19*; *oqxA*; *oqxB*; *aac(6')-Ib-cr*; one-step *gyrA* mutation; *parC* mutation; *mgrB* mutation; *aac(3)-IId; aac(6')-Ib; aadA1*	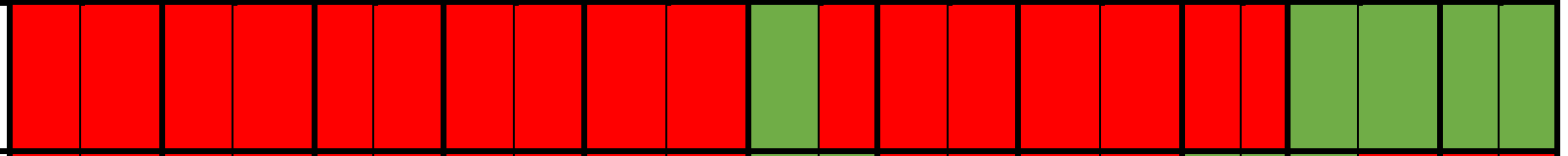
23	*bla*$_{KPC-2}$; *bla*$_{SHV-11}$; *bla*$_{OXA-9}$; *bla*$_{TEM-1}$; *aac(6')-Ib-cr*; *oqxA*; *oqxB*; one-step *gyrA* mutation; *parC* mutation; OmpK35 and OmpK36 truncation; *aac(6')-Ib; aadA2; aac(3)-IVa; aph(4)-Ia; aadA2; aadA1; sul1; sul3; dfrA12*	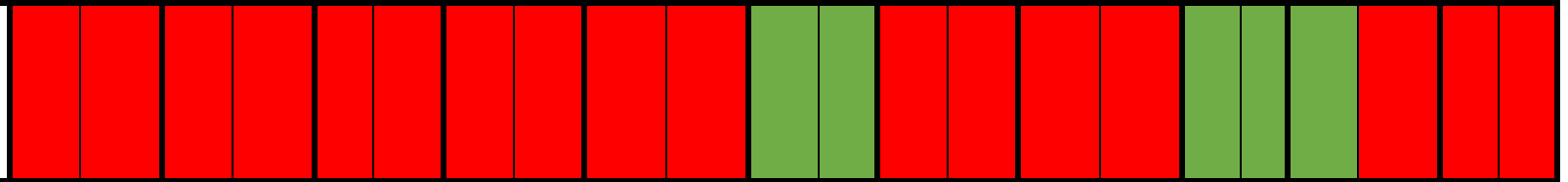
24	*bla*$_{TEM-1}$; *bla*$_{CTX-M-14}$; *bla*$_{DHA-1}$; *bla*$_{SHV-11}$; OmpK36 truncation; *qnrB4*; *oqxA*; *oqxB*; one-step *gyrA* mutation; *tet(A)*;	

	tet(G); *rmtB; aph(3")-Ib; aph(3')-Ia; aac(3)-IId; aph(6)-Id; aph(3)-IId; aadA2; aadA5sul1; sul2*; *dfrA12*; *dfrA1*	
25	bla_{SHV-11}; OmpK36 truncation; *oqxA*; *oqxB*	
26	bla_{SHV-11}; bla_{KPC-2}; *oqxA*; *oqxB*; one-step *gyrA* mutation; *parC* mutation; OmpK35 and OmpK36 truncation; *aac(6')-Ib; aadA2; aadA1; aadA24*	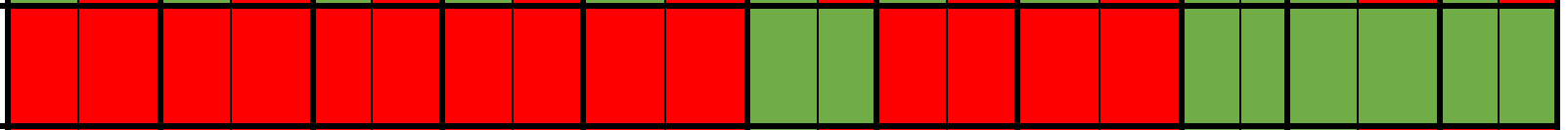
27	bla_{SHV-11}; bla_{TEM-1}; bla_{OXA-9}; bla_{KPC-2}; *oqxA*; *oqxB*; *aac(6')-Ib-cr*; one-step *gyrA* mutation; *parC* mutation; *aph(3')-Ia; aadA2; aac(6')-Ib; sul1; dfrA12*	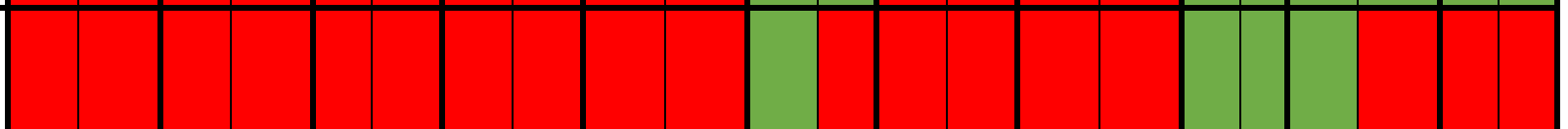
28	bla_{SHV-12}; bla_{TEM-1}; bla_{OXA-9}; bla_{KPC-3}; bla_{SHV-11}; OmpK35 and OmpK36 truncation; *aac(6')-Ib-cr*; *oqxA*; *oqxB*; one-step *gyrA* mutation; *parC* mutation; *aac(6')-Ib; aph(3")-Ib; aadA1*; *sul2*; *dfrA14;* premature stop codon in mgrB	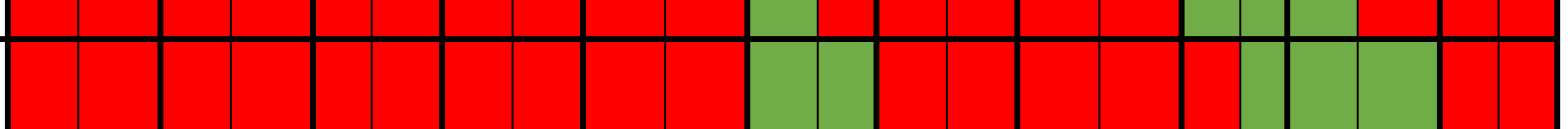
29	bla_{SHV-1}; bla_{NDM-1}; $bla_{CTX-M-15}$; bla_{CMY-4}; OmpK35 truncation; *qnrB1*; *aac(6')-Ib-cr*; *oqxA*; *oqxB*; one-step *gyrA* mutation; *parC* mutation; *rmtf; aacA4; aph(3')-VIa; aadA2*; *sul1*; *dfrA12*	
30	bla_{SHV-11}; bla_{TEM-1}; bla_{OXA-2}; bla_{KPC-3}; OmpK36 truncation; *phoP* mutation; *aac(6')-Ib-cr*; *oqxA*; *oqxB*; *qnrS1*; two-step *gyrA* mutation; *parC* mutation; *aadA8b; aadA1; aadA2; aac(3)-IIa; aacA4; aac(3)-IIa; aacA4; aph(3')-Ia; sul1*; *sul3*; *dfrA12*	
31	$bla_{CTX-M-15}$; bla_{TEM-1}; bla_{SHV-83}; OmpK36 truncation; *oqxA*; *oqxB*; *qnrB1*; *aph(6)-Id; aph(3")-Ib; sul2*; *dfrA14*	
32	bla_{OXA-1}; bla_{SHV-11}; $bla_{CTX-M-15}$; bla_{TEM-1B}; OmpK36 truncation; *oqxA*; *oqxB*; *qnrB1*; *aac(6')-Ib-cr*; *tet(A)*; *aph(6)-Id*; *aph(3")-Ib*; *sul2*; *dfrA14*	

33	*bla*$_{LEN-12}$; *bla*$_{SHV-1}$; OmpK36 truncation; *oqxA*; *oqxB*; *tet(D)*; *sul2*; *dfrA14*																				
34	*bla*$_{SHV-71}$; OmpK36 truncation; *oqxA*; *oqxB*																				
35	*bla*$_{SHV-1}$; OmpK36 truncation; *oqxA*; *oqxB*																				
36	*bla*$_{SHV-36}$; OmpK36 truncation; *oqxA*; *oqxB*; *ant(2")-Ia*																				
37	*bla*$_{TEM-1}$; *bla*$_{KPC-3}$; *bla*$_{SHV-26}$; *bla*$_{SHV-30}$; OmpK36 truncation; *ant(2")-Ia; qnrS1*																				
38	*bla*$_{OKP-B2}$; *bla*$_{TEM-1}$; *bla*$_{SHV-122}$; OmpK36 truncation; *oqxA*; *oqxB*; *tet(D)*; *sul2*; *dfrA26*																				
39	*bla*$_{SHV-62}$; OmpK36 truncation; *oqxA*; *oqxB*																				
40	*bla*$_{SHV-83}$; OmpK36 truncation; *oqxA*; *oqxB*																				
Overall agreement		**85%**		**95%**		**98%**		**85%**		**95%**		**85%**		**95%**		**98%**		**98%**		**80%**	**93%**

213

214

215

216

217

218

219

220

221

222

223

Supplemental Table 4: Average time to detection of resistance genes based on the number of reads detected in minutes

Gene[1]	One copy (minutes)	Ten copies (minutes)	Forty copies (minutes)	Fifty copies (minutes)	One hundred copies (minutes)
β-lactam genes					
Non-ESBL TEM enzymes	0.39 minutes (IQR 0.14-2)	13 minutes (IQR 8-16)	66 minutes (IQR 54-74)	78 minutes (IQR 71-99)	155 minutes (IQR 136-174)
Non-ESBL OXA enzymes	0.91 minutes (IQR 0.6-4.8)	20 minutes (IQR 14-22)	75 minutes (IQR 55-83)	92 minutes (IQR 66-99)	163 minutes (IQR 125-177)
Non-ESBL SHV enzymes	0.6 minutes (IQR 0.1-1.1)	13 minutes (IQR 9-17)	57 minutes (IQR 48-69)	73 minutes (IQR 60-87)	146 minutes (IQR 129-170)
ESBL SHV enzymes	1.1 minutes (IQR 0.03-1.9)	17 copies (IQR 12-17)	57 minutes (IQR 52-63)	74 minutes (IQR 73-75)	125 minutes (IQR 106-139)
ESBL CTX-M-type enzymes	0.5 minutes (IQR 0.14-1.4)	11 minutes (IQR 10-14)	50 minutes (IQR 40-66)	64 minutes (IQR 46-86)	138 minutes (IQR 102-164)
ESBL OXA enzymes	0.58 minutes (IQR 0.1-1.3)	16 minutes (IQR 0.1-0.2)	61 minutes (IQR 55-71)	75 minutes (IQR 72-90)	165 minutes (IQR 148-184)
KPC carbapenemases	0.33 minutes (IQR 0.1-1.1)	12 minutes (IQR 7-14)	57 minutes (IQR 49-71)	74 minutes (IQR 66-90)	150 minutes (IQR 131-169)
NDM carbapenemases	0.7 minutes (IQR 0.01-0.9)	14 minutes (IQR 3-26)	50 minutes (IQR 23-116)	64 minutes (IQR 35-173)	153 minutes (IQR 85-489)
Aminoglycoside inactivating enzymes					
Aminoglycoside modifying enzymes	1.0 minute (IQR 0.3-4)	15 minutes (IQR 9-24)	66 minutes (IQR 50-80)	82 minutes (IQR 61-99)	151 minutes (IQR 130-172)
Ribosomal RNA methyltransferase mutations	0.6 minutes (IQR 0.3-0.9)	12 minutes (IQR 8-15)	55 minutes (IQR 41-69)	70 minutes (IQR 58-81)	132 minutes (IQR 116-148)
Tetracycline resistance genes					
tet(A), tet(B), tet(D), tet(G)	0.9 minutes (IQR 0.4-1.8)	11 minutes (IQR 7-18)	59 minutes (IQR 38-73)	73 minutes (IQR 54-89)	133 minutes (IQR 116-166)
Trimethoprim/sulfamethoxazole related genes					
dfrA genes	0.2 minutes (IQR 0.02-0.5)	14 minutes (IQR 7-16)	68 minutes (IQR 53-75)	85 minutes (IQR 69-92)	164 minutes (IQR 136-180)
sul genes	0.5 minutes (IQR 0.27-1.3)	13 minutes (IQR 7-18)	57 minutes (IQR 45-76)	80 minutes (IQR 65-96)	166 minutes (IQR 131-173)

[1]Only including genes detected in at least three isolates; ESBL: extended-spectrum beta-lactamase

224